

Probabilistic K-means Clustering via Nonlinear Programming

Yujian Li*, Bowen Liu, Zhaoying Liu, and Ting Zhang

Abstract—K-means is a classical clustering algorithm with wide applications. However, soft K-means, or fuzzy c-means at $m = 1$, remains unsolved since 1981. To address this challenging open problem, we propose a novel clustering model, i.e. Probabilistic K-Means (PKM), which is also a nonlinear programming model constrained on linear equalities and linear inequalities. In theory, we can solve the model by active gradient projection, while inefficiently. Thus, we further propose maximum-step active gradient projection and fast maximum-step active gradient projection to solve it more efficiently. By experiments, we evaluate the performance of PKM and how well the proposed methods solve it in five aspects: initialization robustness, clustering performance, descending stability, iteration number, and convergence speed.

Index Terms—K-means, soft K-means, probabilistic K-means, fuzzy c-means, nonlinear programming, active gradient projection, maximum-step active gradient projection, fast maximum-step active gradient projection.



1 INTRODUCTION

CLUSTERING analysis is an unsupervised machine learning method. It has been widely used in image and video processing [1]-[4], speech processing [5], biology [6], medicine [7], sociology [8], and so on. The task of clustering is to find some similarities from datasets [9], [10], and then to classify samples with the similarities into clusters (i.e. classes or categories). Clustering methods mainly include: partition-based clustering [11]-[13], hierarchical-based clustering [14]-[16], density-based clustering [10], [17], [18], graph-based clustering [19]-[21], grid-based clustering [22]-[24], model-based clustering [25]-[27] and subspace clustering [21], [24], [28]-[31], etc. Note that these methods may have intersections.

Partition-based clustering algorithms, such as K-means [11], K-medoids [12], and EM-K-means [32], divide a dataset into several disjoint subsets with a similarity criterion. In general, they first choose initial cluster centers randomly or manually, then adjust categories of samples and update the cluster centers according to the nearest neighbor principle until convergence. Hierarchical-based clustering algorithms fall into two types: bottom-up and top-down. The bottom-up clustering algorithms, such as CURE [14] and BIRCH [15], start with each sample treated as a separate cluster, and repeatedly merge two or more clusters until satisfying certain conditions, e.g. only one cluster left. The top-down clustering algorithms, like MMDCA [16], start with a single cluster of all samples, and repeatedly split one cluster into two or more dissimilar clusters until meeting some criteria,

e.g. only one sample in each cluster. Density-based clustering algorithms, such as DBSCAN [17], affinity propagation [10] and density peak [18], cluster samples according to their density distributions with local centers, where the definition of density may change in different algorithms.

Graph-based clustering algorithms include variational clustering [19], minimum spanning tree [20] and spectral clustering [29], etc. These algorithms construct a similarity graph for a dataset and then find an optimal partition such that the graph has high weights for edges within each group and low weights for edges between different groups. Grid-based clustering algorithms, such as STING [22], WaveCluster [23] and CLIQUE [24], classify datasets with spatial grid cells, which may contain different numbers of data points. Model-based clustering algorithms mainly include self-organizing map (SOM) [25] and statistical clustering [26]. SOM is an unsupervised neural network for projecting all data points onto a two-dimensional plane with similarities between them. Statistical clustering classifies datasets with their probability distributions in optimization of expectation maximization [27].

Subspace clustering algorithms find several subspaces from a data set, where each subspace contains only one cluster. These clustering algorithms may also contain grid-based CLIQUE [24], model-based RAS [26], and graph-based spectral clustering [28]-[31], etc.

K-means clustering algorithms minimize the sum of squared (Euclidean) distances between each sample point and its nearest cluster center, mainly including Lloyd's algorithm [33], Hartigan-Wong's algorithm [34] and MacQueen's algorithm [11]. These heuristic algorithms take advantages of easy implementation, high efficiency and low complexity. However, they are sensitive to initial centers and outliers, and may converge to partitions that are significantly inferior to the global optimum. Meanwhile, they are not suitable for finding non-spherical clusters in a dataset. To improve them, many new algorithms have been proposed, such as GA-K-means, K-means++, K-medoids, L_p -norm K-means,

- Y. Li is with Faculty of Information Technology, Beijing University of Technology, Beijing 100124, China. As corresponding author, he is with School of Artificial Intelligence, Guilin University of Electronic Technology, Guilin 541004, China.
E-mails: liyujian@guet.edu.cn
- B. Liu, Z. Liu and T. Zhang are with Faculty of Information Technology, Beijing University of Technology, Beijing, China, 100124.
E-mail: liubw2017@emails.bjut.edu.cn, zhaoying.liu@bjut.edu.cn, zhangting@bjut.edu.cn

symmetric distance K-means, and kernel K-means. GA-K-means [35] uses a genetic algorithm to select initial centers, and can significantly improve clustering performance on low-dimensional datasets. K-means++ [36] sets initial centers to be far apart data points, and can improve the stability of clustering results. K-medoids [12] replaces mean centers with some special samples called medoids, and can reduce the sensitivity to outliers. L_p -norm K-means [37] exploits Minkowski distance to measure similarities between samples, and can be thought of as an extension of K-means. Symmetric distance K-means [38] employs a non-metric point symmetric distance for clustering, and can find different-shape clusters. Kernel K-means [39] selects a kernel function to cluster in a feature space, and can find non-linear separable structures. Ref. [40] extends K-means type algorithms by integrating both intracluster compactness and intercluster separation.

Another well-known variant of K-means is fuzzy c-means (FCM) [13] proposed by Bezdek in 1981. FCM determines partitions by computing the membership degree to each cluster for each data point. The higher the membership degree of a data point to a cluster, the greater possibility the data point belongs to the cluster. Compared with K-means, FCM is more flexible in applications, but with one more parameter m to be selected manually. In theory, m ranges from 1 to infinity. In practice, $m \approx 1.3$ is a relatively good value for clustering [41]. As m approaches 1, FCM degenerates to K-means, with all membership degrees converging to 0 or 1. Additionally, FCM has many variants, such as possibilistic c-means [42], sparse possibilistic c-means [43], and size insensitive integrity-based FCM [44]. However, a remaining problem is how to solve FCM at $m = 1$. The problem will be solved by a novel clustering model, called probabilistic K-means (PKM).

In fact, PKM is an equivalent model to FCM at $m = 1$. Theoretically, PKM is also a nonlinear programming problem with many constraints of linear equalities and linear inequalities. It can be solved by an active gradient projection (AGP) method, i.e. a combination of active set [45] and gradient projection [46], [47]. To speed up the AGP method, we further present a maximum-step AGP (MSAGP) method by iteratively computing maximum feasible step length and a fast MSAGP (FMSAGP) method by efficiently computing projection matrices. Also, we evaluate the performance of PKM and how well the proposed methods solve it on artificial and real datasets.

The remainder of this paper is organized as follows: Section 2 introduces K-means, fuzzy c-means and probabilistic K-means. Section 3 presents solutions to PKM in detail. Experimental results are reported in Section 4. Finally, conclusions are drawn in Section 5.

2 PKM CLUSTERING MODEL

Given a set of data points $\mathbf{X} = \{\mathbf{x}_i | \mathbf{x}_i \in \mathbb{R}^D, 1 \leq i \leq L\}$, let us divide it into K clusters. Suppose ω_j is the j -th cluster. Then, $\mathbf{X} = \bigcup_{j=1}^K \omega_j, \forall 1 \leq i \neq j \leq K, \omega_i \cap \omega_j = \emptyset$. If L_j denotes the number of elements in ω_j with the center of

\mathbf{c}_j , and $L = \sum_{j=1}^K L_j$, then the standard K-means clustering model is described as minimizing a hard objective function:

$$J = \sum_{i=1}^K \sum_{\mathbf{x}_i \in \omega_j} \|\mathbf{x}_i - \mathbf{c}_j\|^2 \quad (1)$$

where

$$\mathbf{c}_j = \frac{1}{L_j} \sum_{\mathbf{x}_i \in \omega_j} \mathbf{x}_i \quad (2)$$

With membership degree w_{ij} assigned to the i -th data point in the j -th cluster for $1 \leq i \leq L$ and $1 \leq j \leq K$, the hard K-means model is extended to a soft model, namely the FCM model. FCM minimizes the objective function below:

$$\begin{aligned} J &= \sum_{j=1}^K \sum_{i=1}^L w_{ij}^m \|\mathbf{x}_i - \mathbf{c}_j\|^2 \\ \text{s.t. } &\sum_{j=1}^K w_{ij} = 1, w_{ij} \geq 0 \end{aligned} \quad (3)$$

where m ranges from 1 to infinity.

When $m > 1$, w_{ij} and \mathbf{c}_j can be computed alternately as follows [13]

$$\begin{cases} w_{ij} = \frac{\|\mathbf{x}_i - \mathbf{c}_j\|^{-\frac{2}{m-1}}}{\sum_{k=1}^K \|\mathbf{x}_i - \mathbf{c}_k\|^{-\frac{2}{m-1}}} \\ \mathbf{c}_j = \frac{\sum_{i=1}^L w_{ij}^m \mathbf{x}_i}{\sum_{i=1}^L w_{ij}^m} \end{cases} \quad (4)$$

However, FCM at $m = 1$ is an challenging open problem that remains unsolved since 1981. It is also called "soft K-means". Replacing membership degree w_{ij} by probability p_{ij} , we get the soft K-means clustering model as follows,

$$\begin{aligned} J &= \sum_{j=1}^K \sum_{i=1}^L p_{ij} \|\mathbf{x}_i - \mathbf{c}_j\|^2 \\ \text{s.t. } &\sum_{j=1}^K p_{ij} = 1, p_{ij} \geq 0 \end{aligned} \quad (5)$$

Note that probability p_{ij} takes a value in $[0, 1]$. This means that data point \mathbf{x}_i may belong to class j with probability p_{ij} , rather than to only one class in hard K-means. The higher the probability p_{ij} , the more likely that \mathbf{x}_i is in class j . The view of probability is more in line with Bayesian decision theory [48].

For the soft K-means, we can construct a Lagrangian function,

$$J = \sum_{j=1}^K \sum_{i=1}^L p_{ij} \|\mathbf{x}_i - \mathbf{c}_j\|^2 + \sum_{i=1}^L \lambda_i \left(\sum_{j=1}^K p_{ij} - 1 \right) \quad (6)$$

Letting $\frac{\partial J}{\partial \mathbf{c}_j} = \sum_{i=1}^K \sum_{i=1}^L 2p_{ij}(\mathbf{c}_j - \mathbf{x}_i) = 0$, we obtain

$$\mathbf{c}_j = \frac{\sum_{i=1}^L p_{ij} \mathbf{x}_i}{\sum_{i=1}^L p_{ij}} \quad (7)$$

Substituting (7) into (5), we get an equivalent model, namely, PKM

$$J = \sum_{j=1}^K \sum_{i=1}^L p_{ij} \left\| \mathbf{x}_i - \frac{\sum_{i=1}^L p_{ij} \mathbf{x}_i}{\sum_{i=1}^L p_{ij}} \right\|^2 \quad (8)$$

$$s.t. \sum_{j=1}^K p_{ij} = 1, p_{ij} \geq 0$$

If setting $K = 2$ and $L = 2$ with $\mathbf{x}_1 = (1, 1)^T$, $\mathbf{x}_2 = (2, 2)^T$, we can rewrite the objective function as follows,

$$\begin{aligned} J(p_{11}, p_{12}, p_{21}, p_{22}) &= \sum_{j=1}^2 \sum_{i=1}^2 p_{ij} \left\| \mathbf{x}_i - \frac{\sum_{i=1}^2 p_{ij} \mathbf{x}_i}{\sum_{i=1}^2 p_{ij}} \right\|^2 \\ &= \left[p_{11} \left\| \frac{p_{21} \mathbf{x}_1 - p_{21} \mathbf{x}_2}{p_{11} + p_{21}} \right\|^2 + p_{21} \left\| \frac{p_{11} \mathbf{x}_2 - p_{11} \mathbf{x}_1}{p_{11} + p_{21}} \right\|^2 \right] \\ &+ \left[p_{12} \left\| \frac{p_{22} \mathbf{x}_1 - p_{22} \mathbf{x}_2}{p_{12} + p_{22}} \right\|^2 + p_{22} \left\| \frac{p_{12} \mathbf{x}_2 - p_{12} \mathbf{x}_1}{p_{12} + p_{22}} \right\|^2 \right] \\ &= \frac{p_{11} p_{12} + p_{21} p_{22}}{(p_{11} + p_{21})(p_{12} + p_{22})} \|\mathbf{x}_1 - \mathbf{x}_2\|^2 \\ &= \frac{p_{11}(1 - p_{11}) + p_{21}(1 - p_{21})}{(p_{11} + p_{21})(2 - p_{11} - p_{21})} \|\mathbf{x}_1 - \mathbf{x}_2\|^2 \\ &= \frac{p_{11} + p_{21} - p_{11}^2 - p_{21}^2}{(p_{11} + p_{21})(2 - p_{11} - p_{21})} \|\mathbf{x}_1 - \mathbf{x}_2\|^2 = J(p_{11}, p_{21}), \end{aligned} \quad (9)$$

where $p_{12} = 1 - p_{11}$ ($0 \leq p_{11} \leq 1$) and $p_{22} = 1 - p_{21}$ ($0 \leq p_{21} \leq 1$).

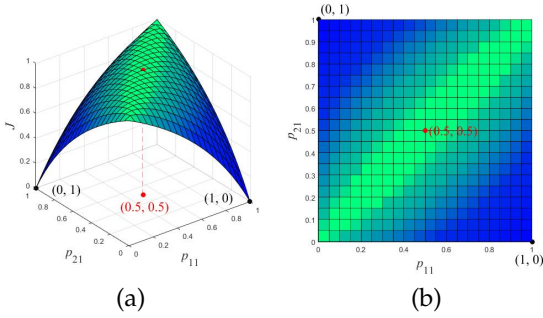


Fig. 1. A surface of $J(p_{11}, p_{21})$ (a), and its vertical view (b).

Therefore, $J(p_{11}, p_{12}, p_{21}, p_{22}) = J(p_{11}, p_{21})$ is indeed a function of p_{11} and p_{21} , as shown in Fig. 1. Note that Fig. 1a is a surface of $J(p_{11}, p_{21})$, with its vertical view in Fig. 1b. In Fig. 1, p_{11} is the probability of \mathbf{x}_1 in cluster 1, and p_{21} is the probability of \mathbf{x}_2 in cluster 1. Obviously, the function $J(p_{11}, p_{21})$ has countless probability pairs that take the same maximum value of 1, satisfying $p_{11} = p_{21}$, e.g. (0.5, 0.5). But it has only two probability pairs that take the same minimum value of 0, namely (0, 1) or (1, 0). Because of symmetricity, the two pairs produce the same cluster assignment: \mathbf{x}_1 in one class, and \mathbf{x}_2 in the other.

3 SOLUTIONS TO PKM

According to (8), PKM is a nonlinear programming problem constrained on linear equalities and linear inequalities. In

theory, the problem can be solved by AGP, but requiring optimization of step length and fast computation of projection matrices.

In this section, we first calculate the gradient of PKM's objective function, and then propose the AGP method and its two improvements: the MSAGP method and the FM-SAGP method, to solve the PKM model.

3.1 Gradient Calculation

For convenience, we define F_k as

$$F_k = \left\| \mathbf{x}_k - \frac{\sum_{i=1}^L p_{ij} \mathbf{x}_i}{\sum_{i=1}^L p_{ij}} \right\|^2 \quad (10)$$

Using the chain rule on (8), we obtain

$$\frac{\partial J}{\partial p_{ij}} = F_i + \sum_{k=1}^L p_{kj} \frac{\partial F_k}{\partial p_{ij}} \quad (11)$$

According to (10), we can further derive (12)-(15) as follows,

$$\begin{aligned} \frac{\partial F_k}{\partial p_{ij}} &= \frac{\partial}{\partial p_{ij}} \left[\mathbf{x}_k^T \mathbf{x}_k - \mathbf{x}_k^T \left(\frac{\sum_{i=1}^L p_{ij} \mathbf{x}_i}{\sum_{i=1}^L p_{ij}} \right) \right. \\ &\quad \left. - \left(\frac{\sum_{i=1}^L p_{ij} \mathbf{x}_i}{\sum_{i=1}^L p_{ij}} \right)^T \mathbf{x}_k + \left(\frac{\sum_{i=1}^L p_{ij} \mathbf{x}_i}{\sum_{i=1}^L p_{ij}} \right)^T \left(\frac{\sum_{i=1}^L p_{ij} \mathbf{x}_i}{\sum_{i=1}^L p_{ij}} \right) \right] \end{aligned} \quad (12)$$

$$\begin{aligned} \frac{\partial F_k}{\partial p_{ij}} &= -2 \frac{\mathbf{x}_k^T \mathbf{x}_i \sum_{i=1}^L p_{ij} - \mathbf{x}_k^T \sum_{i=1}^L p_{ij} \mathbf{x}_i}{\left(\sum_{i=1}^L p_{ij} \right)^2} \\ &+ 2 \frac{\mathbf{x}_i^T \left(\sum_{i=1}^L p_{ij} \mathbf{x}_i \right) \sum_{i=1}^L p_{ij} - \left[\left(\sum_{i=1}^L p_{ij} \mathbf{x}_i^T \right) \sum_{i=1}^L p_{ij} \mathbf{x}_i \right]}{\left(\sum_{i=1}^L p_{ij} \right)^3} \end{aligned} \quad (13)$$

$$\begin{aligned} \frac{\partial F_k}{\partial p_{ij}} &= \frac{-2}{\sum_{i=1}^L p_{ij}} \left(\mathbf{x}_k^T \mathbf{x}_i - \frac{\mathbf{x}_k^T \sum_{i=1}^L p_{ij} \mathbf{x}_i}{\sum_{i=1}^L p_{ij}} \right) \\ &- \frac{\mathbf{x}_i^T \left(\sum_{i=1}^L p_{ij} \mathbf{x}_i \right)}{\sum_{i=1}^L p_{ij}} + \frac{\left[\left(\sum_{i=1}^L p_{ij} \mathbf{x}_i^T \right) \sum_{i=1}^L p_{ij} \mathbf{x}_i \right]}{\left(\sum_{i=1}^L p_{ij} \right)^2} \end{aligned} \quad (14)$$

$$\frac{\partial F_k}{\partial p_{ij}} = -\frac{2}{\sum_{i=1}^L p_{ij}} \left(\mathbf{x}_k - \frac{\sum_{i=1}^L p_{ij} \mathbf{x}_i}{\sum_{i=1}^L p_{ij}} \right)^T \left(\mathbf{x}_i - \frac{\sum_{i=1}^L p_{ij} \mathbf{x}_i}{\sum_{i=1}^L p_{ij}} \right) \quad (15)$$

Substituting (15) into (11), we finally get,

$$\frac{\partial J}{\partial p_{ij}} = \left\| \mathbf{x}_i - \frac{\sum_{i=1}^L p_{ij} \mathbf{x}_i}{\sum_{i=1}^L p_{ij}} \right\|^2 - \frac{2}{\sum_{i=1}^L p_{ij}} \sum_{k=1}^L p_{kj} \left(\mathbf{x}_k - \frac{\sum_{i=1}^L p_{ij} \mathbf{x}_i}{\sum_{i=1}^L p_{ij}} \right)^T \left(\mathbf{x}_i - \frac{\sum_{i=1}^L p_{ij} \mathbf{x}_i}{\sum_{i=1}^L p_{ij}} \right) \quad (16)$$

$$\frac{\partial J}{\partial p_{ij}} = \left[\left(\mathbf{x}_i - \frac{\sum_{i=1}^L p_{ij} \mathbf{x}_i}{\sum_{i=1}^L p_{ij}} \right) - \frac{2}{\sum_{i=1}^L p_{ij}} \sum_{k=1}^L p_{kj} \left(\mathbf{x}_k - \frac{\sum_{i=1}^L p_{ij} \mathbf{x}_i}{\sum_{i=1}^L p_{ij}} \right) \right]^T \left(\mathbf{x}_i - \frac{\sum_{i=1}^L p_{ij} \mathbf{x}_i}{\sum_{i=1}^L p_{ij}} \right) \quad (17)$$

and the gradient

$$\nabla J = \begin{bmatrix} \frac{\partial J}{\partial p_{11}} & \dots & \frac{\partial J}{\partial p_{1K}} & \dots \\ \frac{\partial J}{\partial p_{ij}} & \dots & \frac{\partial J}{\partial p_{Lj}} & \dots & \frac{\partial J}{\partial p_{LK}} \end{bmatrix} \quad (18)$$

3.2 The AGP Method

In the constraints of PKM, there are L equalities and KL inequalities,

$$\forall 1 \leq i \leq L, \sum_{j=1}^K p_{ij} = 1 \quad (19)$$

$$\forall 1 \leq i \leq L, 1 \leq j \leq K, p_{ij} \geq 0 \quad (20)$$

where probability matrix $(p_{ij})_{L \times K}$ can be vectorized as

$$\mathbf{P} = [p_{11} \dots p_{1K} \dots p_{ij} \dots p_{Lj} \dots p_{LK}]^T \quad (21)$$

Let $\mathbf{I}_{LK \times LK}$ be the identity matrix of size $LK \times LK$. Define two matrices, inequality matrix \mathbf{A} and equality matrix \mathbf{E} ,

$$\mathbf{A} = \mathbf{I}_{LK \times LK} \quad (22)$$

$$\mathbf{E} = \begin{bmatrix} \underbrace{1 \dots 1}_K & 0 & 0 & \dots & 0 & 0 & 0 \\ 0 & \dots & 0 & \dots & 0 & \dots & 0 \\ \underbrace{0 \dots 0}_K & \underbrace{1 \dots 1}_K & \dots & \dots & \dots & \dots & \dots \\ 0 & 0 & \dots & 0 & 0 & 0 & \underbrace{1 \dots 1}_K \end{bmatrix}_{L \times LK} \quad (23)$$

Obviously, each row of \mathbf{A} corresponds to one and only one inequality in (20). Moreover, each row of \mathbf{E} corresponds to one and only one equality in (19). Accordingly, the PKM's constraints, namely, (19)-(20), can be simply expressed as

$$\mathbf{A}\mathbf{P} \geq \mathbf{0}, \mathbf{E}\mathbf{P} = \mathbf{1} \quad (24)$$

Let $\mathbf{P}^{(0)}$ stand for an initial probability vector, and $\mathbf{P}^{(k)}$ for the probability vector at iteration k . Note that $\mathbf{P}^{(0)}$ is randomly initialized with the constraints of (24). At iteration k , the rows of inequality matrix \mathbf{A} are broken into two groups: one is active, the other is inactive. The active group is composed of all inequalities that must work exactly as an equality at $\mathbf{P}^{(k)}$, whereas the inactive group is composed of the left inequalities. If $\mathbf{A}_1^{(k)}$ and $\mathbf{A}_2^{(k)}$ respectively denote the active group and the inactive group, we have

$$\mathbf{A}_1^{(k)} \mathbf{P}^{(k)} = \mathbf{0} \quad (25)$$

$$\mathbf{A}_2^{(k)} \mathbf{P}^{(k)} > \mathbf{0} \quad (26)$$

Combining $\mathbf{A}_1^{(k)}$ with \mathbf{E} , we define an active matrix $\mathbf{N}^{(k)}$, namely,

$$\mathbf{N}^{(k)} = \begin{bmatrix} \mathbf{A}_1^{(k)} \\ \mathbf{E} \end{bmatrix} \quad (27)$$

which determines the active constraints at iteration k .

When $\mathbf{N} = \mathbf{N}^{(k)}$ is not a square matrix, we construct two matrices $\mathbf{G}^{(k)}$ and $\mathbf{Q}^{(k)}$ as follows,

$$\mathbf{G}^{(k)} = \mathbf{N}^T (\mathbf{N}\mathbf{N}^T)^{-1} \mathbf{N} \quad (28)$$

$$\mathbf{Q}^{(k)} = \mathbf{I}_{LK \times LK} - \mathbf{G}^{(k)} \quad (29)$$

where $\mathbf{G}^{(k)}$ is called projection matrix, and $\mathbf{Q}^{(k)}$ is its orthogonal projection matrix [46].

At iteration k , projecting the gradient of PKM's objective function on the subspace of the active constraints, we obtain the projected gradient,

$$\mathbf{d}^{(k)} = -\mathbf{Q}^{(k)} \nabla J(\mathbf{P}^{(k)}) \quad (30)$$

If $\mathbf{d}^{(k)} = \mathbf{0}$, we stop at a local minimum. Otherwise, we compute the probability vector at iteration $k+1$,

$$\mathbf{P}^{(k+1)} = \mathbf{P}^{(k)} + t \mathbf{d}^{(k)} \quad (31)$$

where t is a step length. Usually, t takes a small value, e.g. $t = 0.01$ or $t = 0.1$.

When $\mathbf{N} = \mathbf{N}^{(k)}$ is a square matrix, \mathbf{N} must be invertible. Meanwhile, the projection matrix $\mathbf{G}^{(k)} = \mathbf{N}^T (\mathbf{N}\mathbf{N}^T)^{-1} \mathbf{N} = \mathbf{I}_{LK \times LK}$, and $\mathbf{Q}^{(k)} = \mathbf{0}$. Thus, the projected gradient $\mathbf{d}^{(k)} = -\mathbf{Q}^{(k)} \nabla J(\mathbf{P}^{(k)}) = \mathbf{0}$, which cannot be chosen as a descent direction. Based on [47], we find the descent direction as follows.

1) Compute a new vector,

$$\mathbf{q}^{(k)} = (\mathbf{N}\mathbf{N}^T)^{-1} \mathbf{N} \nabla J = (\mathbf{N}^T)^{-1} \nabla J \quad (32)$$

2) Break $\mathbf{q}^{(k)}$ into two parts $\mathbf{q}_1^{(k)}$ and $\mathbf{q}_2^{(k)}$, namely,

$$\mathbf{q}^{(k)} = \begin{bmatrix} \mathbf{q}_1^{(k)} \\ \mathbf{q}_2^{(k)} \end{bmatrix} = \begin{bmatrix} (\mathbf{q}_1^{(k)})^T & (\mathbf{q}_2^{(k)})^T \end{bmatrix}^T \quad (33)$$

where the size of $\mathbf{q}_1^{(k)}$ is the number of rows of $\mathbf{A}_1^{(k)}$, and that of $\mathbf{q}_2^{(k)}$ is the number of rows of \mathbf{E} .

3) If all elements of $\mathbf{q}_1^{(k)}$ are greater than or equal to 0, i.e. $\mathbf{q}_1^{(k)} \geq \mathbf{0}$, then stop. Otherwise, choose any one that is less than 0, delete the corresponding row of $\mathbf{A}_1^{(k)}$, and use (27)-(30) to compute $\mathbf{d}^{(k)}$.

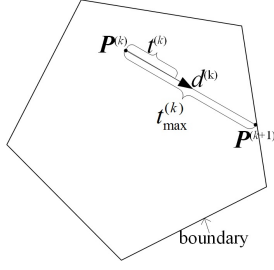


Fig. 2. A comparison of step length $t^{(k)}$ for AGP and $t_{\max}^{(k)}$ for MSAGP.

3.3 The MSAGP Method

In the AGP method, the step length is manually chosen as a small number, leading to slow convergence. To address this issue, we present the MSAGP method by iteratively estimating the maximum step length in the feasible region. At iteration k , because $A_1^{(k)}P^{(k)} = \mathbf{0}$ and $A_2^{(k)}P^{(k)} > \mathbf{0}$, we can estimate the maximum step length

$$t^{(k)} = t_{\max}^{(k)} \quad (34)$$

as follows.

- 1) Let $p_{ij}^{(k+1)} = p_{ij}^{(k)} + t_{ij}d_{ij}^{(k)} = 0$ for $p_{ij}^{(k)} > 0$,
- 2) Compute $t_{ij} = -\frac{p_{ij}^{(k)}}{d_{ij}^{(k)}}$ for $p_{ij}^{(k)} > 0$ and $d_{ij}^{(k)} < 0$,
- 3) $t_{\max}^{(k)} = \min\{t_{ij}\}$.

In Fig. 2, we can see that step length $t^{(k)}$ for AGP is shorter than $t_{\max}^{(k)}$ for MSAGP at iteration k . Thus, MSAGP is expected to converge faster than AGP because it always finds a boundary point $P^{(k+1)}$ to update probability vector $P^{(k)}$. The faster convergence will be confirmed in Section 4.

3.4 The FMSAGP Method

Although MSAGP converges faster than AGP, it has to calculate a large number of matrix inversions. In fact, according to (28), the calculation of $G^{(k)} = N^T(NN^T)^{-1}N$ iteratively requires $(NN^T)^{-1}$ with $N = N^{(k)}$. To calculate $G^{(k)}$ more efficiently, it needs the following lemma.

Lemma. Suppose that \mathbf{n} is a row vector and $[\mathbf{n}^T, N^T]^T$ is full row rank. If projection matrix $G_N = N^T(NN^T)^{-1}N$ and its orthogonal projection matrix $Q_N = I - G_N$, then

$$G_{(\mathbf{n}^T, N^T)^T} = G_N + Q_N \mathbf{n}^T \langle Q_N \mathbf{n}^T, Q_N \mathbf{n}^T \rangle^{-1} \mathbf{n} Q_N. \quad (35)$$

Proof. Because $[\mathbf{n}^T, N^T]^T$ is full row rank, by matrix theory [49]-[51], there must exist a matrix G such that

$$\begin{cases} G_{(\mathbf{n}^T, N^T)^T} = G + G_N, \\ GG_N = G_N G = \mathbf{0} \end{cases}, \quad (36)$$

Meanwhile, there must exist a matrix Z , such that

$$G = Z^T \mathbf{n}^T \langle Z^T \mathbf{n}^T, Z^T \mathbf{n}^T \rangle^{-1} \mathbf{n} Z \quad (37)$$

Combining (36) with (37), we obtain

$$Z^T \mathbf{n}^T \langle Z^T \mathbf{n}^T, Z^T \mathbf{n}^T \rangle^{-1} \mathbf{n} Z G_N = \mathbf{0} \quad (38)$$

Thus, $\mathbf{n} Z G_N = \mathbf{0}$ must hold for all \mathbf{n} . This leads to $Z G_N = \mathbf{0}$. That is to say, Z is the orthogonal projection matrix of G_N , $Z = I - G_N = Q_N$. Moreover, both G_N and Q_N are symmetric matrices. Hence, (35) holds.

Using the above lemma, we can devise the FMSAGP method as follows,

- 1) Let $k = 0$, $N = N^{(0)} = E$, $G^{(0)} = N^T(NN^T)^{-1}N$, initialize $P^{(0)}$, go to 4);
- 2) Find an active row vector \mathbf{n} from $A_2^{(k-1)}$, such that $\mathbf{n}^T P^{(k-1)} > \mathbf{0}$, $\mathbf{n}^T P^{(k)} = \mathbf{0}$;
- 3) Compute $G^{(k)}$ as

$$G^{(k)} = G^{(k-1)} + Q^{(k-1)} \mathbf{n}^T \langle Q^{(k-1)} \mathbf{n}^T, Q^{(k-1)} \mathbf{n}^T \rangle^{-1} \mathbf{n} Q^{(k-1)} \quad (39)$$

- 4) Compute $Q^{(k)} = I_{LK \times LK} - G^{(k)}$, and $d^{(k)} = -Q^{(k)} \nabla J(P^{(k)})$;
- 5) Compute step length $t^{(k)}$ by (34) and probability vector $P^{(k+1)}$ by (31);
- 6) Let $k = k + 1$, if $G^{(k)} \neq I_{LK \times LK}$, go to 2);
- 7) Construct $N = N^{(k)}$ by (27), and compute a new vector $\mathbf{q}^{(k)} = (N^T)^{-1} \nabla J$ by (32);
- 8) Break $\mathbf{q}^{(k)}$ into two parts $\mathbf{q}_1^{(k)}$ and $\mathbf{q}_2^{(k)}$ by (33);
- 9) If all elements of $\mathbf{q}_1^{(k)}$ are greater than or equal to 0, stop;
- 10) Choose any element less than 0 from $\mathbf{q}_1^{(k)}$, and delete the corresponding row of $A_1^{(k)}$;
- 11) Reconstruct $N = N^{(k)}$ by (27);
- 12) Compute $d^{(k)}$ by (28)-(30), $t^{(k)}$ by (34), and $P^{(k+1)}$ by (31);
- 13) Let $k = k + 1$, and go to 7).

4 EXPERIMENTS

In order to evaluate the performance of PKM and how well the methods of AGP, MSAGP, and FMSAGP solve it, we conduct a large number of experiments on fifteen datasets: one artificial dataset, one human face dataset, and thirteen UCI datasets. These datasets are detailed in Table 1.

TABLE 1
Details of Artificial and Benchmark Datasets.

	Instance	Class	Dimension
Artificial dataset	310	4	2
Yale-faces-B	5850	10	1200
UCI	Iris	150	3
	Parkinson	195	2
	Seeds	210	3
	Segmentation	210	7
	Glass	214	6
	Ionosphere	351	2
	Dermatology	358	6
	Breast-cancer	683	2
	Natural	2000	9
	Yeast	2426	3
	Waveform	5000	3
	Satellite	6435	6
	Epileptic	11500	5

The artificial dataset is generated by ourselves. As shown in Fig. 3, it is composed of 310 data points, with 150, 150, 5 and 5 respectively from 4 classes. The human face dataset is Yale-faces-B¹, which consists of 5850 images scaled down to

1. https://cervisia.org/machine_learning_data.php

TABLE 2
Initialization robustness of PKM, KM++ and FCM on the artificial dataset.

	PKM	KM++	FCM ($m = 1.05, 1.09, 1.1, 1.3, 1.4, 1.5, 1.9, 2.0, 2.1$)								
			1.05	1.09	1.1	1.3	1.4	1.5	1.9	2.0	2.1
Correct times	954	645	—	687	693	780	691	0	0	0	0
Correct percentage	95.4%	64.5%	—	68.7%	69.3%	78.0%	69.1%	0	0	0	0

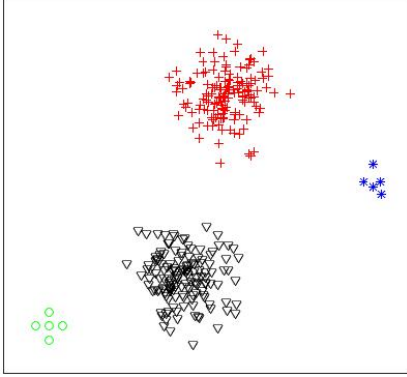


Fig. 3. Original distribution of the artificial dataset with 4 classes.

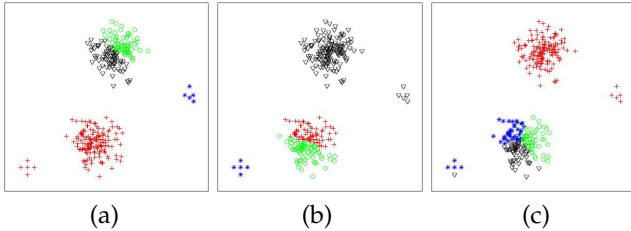


Fig. 4. Three inconsistent distributions with the artificial dataset.

30×40 pixels, with each saved as a 1200-dimensional vector. The thirteen UCI datasets are selected from UCI Machine Learning Repository², including Iris, Parkinson, Seeds, Segmentation, Glass, Ionosphere, Dermatology, Breast-cancer, Natural, Yeast, Waveform, Satellite, and Epileptic.

All experiments are carried out on the same computer (i7-4790 CPU, 3.60GHz, 8.00G RAM), running Windows 7 and Matlab 2015a. The results of FCM are obtained by Matlab's build-in function "fcm". The results of K-means++ (KM++) are obtained by Matlab's build-in function "kmeans". The results of PKM are obtained by Matlab implementation of AGP, MSAGP and FMSAGP, using two build-in functions "sparse" and "full" for matrix optimization.

The experiments are organized and analyzed in five aspects: initialization robustness, clustering performance, descent stability, iteration number, and convergence speed. The first two respects are used to evaluate the performance of PKM, and the last three respects are used to evaluate how well the methods of AGP, MSAGP, and FMSAGP solve PKM.

4.1 Initialization Robustness

In this subsection, we evaluate initialization robustness of PKM, KM++ and FCM on the artificial dataset, with the result given in Table 2. The initialization robustness is defined as the number of correct times out of running an algorithm 1000 times initialized randomly. The correctness means the cluster assignment of a dataset is completely consistent with its original distribution. With the artificial dataset in Fig. 3, three inconsistent distributions are displayed as examples in Fig. 4. From Table 2, we can see that PKM have 954 correct times, more than 645 by KM++. However, FCM may have number of correct times that varies with parameter m . For example, it has 687, 693, 780 and 691 correct times at $m = 1.09, 1.1, 1.3$ and 1.4 , respectively. However, it has no correct times at $m = 1.5, 1.09, 2.0$ and 2.1 . At $m = 1.3$, FCM achieves the maximum number of correct times, namely 780, still lower than PKM.

Overall, PKM has a correct percentage of 95.4%, better than KM++ (64.5%) and FCM (0 to 78.0%) in terms of initialization robustness.

4.2 Clustering Performance

In this subsection, we evaluate clustering performance of PKM, KM++ and FCM in terms of five measures: Standard Squared Error (SSE), Davies Bouldin Index (DBI) [52], Normalized Mutual Information (NMI) [53], Adjusted Rand Index (ARI) [53], and V-measure (VM) [54]. The SSE is defined as

$$SSE = \sum_{i=1}^K \sum_{x_i \in \omega_j} \|x_i - c_j\|^2 \quad (40)$$

where K is the number of clusters, and c_j is the center (mean) of the j -th cluster. DBI is the ratio of within-class distances to between-class distances. NMI is a normalization of the mutual information score to scale the results between 0 (no mutual information) and 1 (perfect correlation). ARI is an adjusted similarity measure between two clusters. V-measure is a harmonic mean between homogeneity and completeness, where homogeneity means that each cluster is a subset of a single class, and completeness means that each class is a subset of a single cluster.

The above five measures fall into two types: internal evaluation and external evaluation. Internal evaluation, including SSE and DBI, can work without ground truth labels. But external evaluation, such as NMI, ARI and VM, must work with ground truth labels. The lower the internal evaluation, the better the clustering result. However, the higher the external evaluation, the better the clustering result.

We test PKM (solved by FMSAGP), KM++ and FCM ($m = 1.3$) on Yale-faces-B and 13 UCI datasets, with the 5-time average results reported in Table 3. The best in each

2. <http://archive.ics.uci.edu/ml>

TABLE 3
Internal Evaluation of PKM, KM++ and FCM ($m = 1.3$).

Datasets	SSE			DBI		
	PKM	KM++	FCM	PKM	KM++	FCM
Yale-faces-B	8.51e9	8.52e9	8.42e9	1.6184	1.6128	1.5986
Iris	78.942	110.89	110.9	0.3928	0.4801	0.4561
Seeds	587.05	588.05	587.32	0.3980	0.4421	0.3962
Breast-cancer	2419.3	2419.3	2419.3	0.3785	0.3786	0.3786
Dermatology	11702	11702	11702	0.7180	0.7939	0.7609
Ionosphere	2419.4	2419.4	2419.4	0.7567	0.7567	0.7579
Parkinson	1.34e6	1.34e6	1.34e6	0.4932	0.4974	0.4974
Glass	372.77	379.41	366.35	0.8505	0.7074	0.7909
Natural	1888.3	1883.5	1879.2	1.7035	1.6587	1.6089
Satellite	1.67e7	1.69e7	1.69e7	0.8524	0.8731	0.8957
Yeast	713.89	713.88	714.07	1.1601	1.1582	1.1753
Segmentation	1.01e6	9.85e5	1.99e6	0.7461	0.7530	1.0899
Waveform	1.33e5	1.33e5	1.33e5	0.8663	0.9301	0.8665
Epileptic	5.1e10	5.1e10	5.3e10	2.6051	2.6956	3.6407

case is highlighted in bold. Some big values are in scientific notation. For instance, 8.42e9 means 8.42×10^9 .

From Table 3, we have the following observations.

1) By SSE, PKM performs better than KM++ on 5 datasets, and as well as KM++ on 6 datasets. Meanwhile, it performs better than FCM on 6 datasets, and as well as FCM on 5 datasets.

2) By DBI, PKM performs better than KM++ on 9 datasets, and as well as KM++ on 1 datasets. Meanwhile, it performs better than FCM on 10 datasets.

From Table 4, we have the following observations.

1) By NMI, PKM performs better than KM++ on 5 datasets, and as well as KM++ on 5 datasets. Meanwhile, it outperforms FCM on 12 datasets.

2) By ARI, PKM perform better than KM++ on 5 datasets, and as well as KM++ on 4 datasets. Meanwhile, it outperforms FCM on 11 datasets.

3) By VM, PKM perform better than KM++ on 9 datasets, and as well as KM++ on 2 datasets. Meanwhile, it outperforms FCM on 11 datasets.

Overall, PKM outperforms KM++ and FCM in terms of SSE, DBI, NMI, ARI and VM.

4.3 Descent Stability of MSAGP

In this subsection, we evaluate the descent stability of MSAGP. Theoretically, AGP needs a small step length to make the value of its objective function stably descend at each iteration and gradually converge to a local minimum. If the step length is too large, the value may descend with oscillation, and even does not converge at all. MSAGP iteratively estimates a maximum step length for AGP in the feasible region of PKM so as to speed up its convergence with fewer iterations. However, will this estimate have any serious influence of oscillation on the convergence of AGP?

To demonstrate the influence, we select 9 UCI datasets from Table 1, including Satellite, Yale, Epileptic, Natural, Yeast, Waveform, Glass, Dermatology, and Breast-cancer. On these datasets, we use MSAGP to solve PKM, and illustrate the value of its objective function vs. iteration in Fig. 5.

Obviously, we can see that MSAGP descends stably without oscillation.

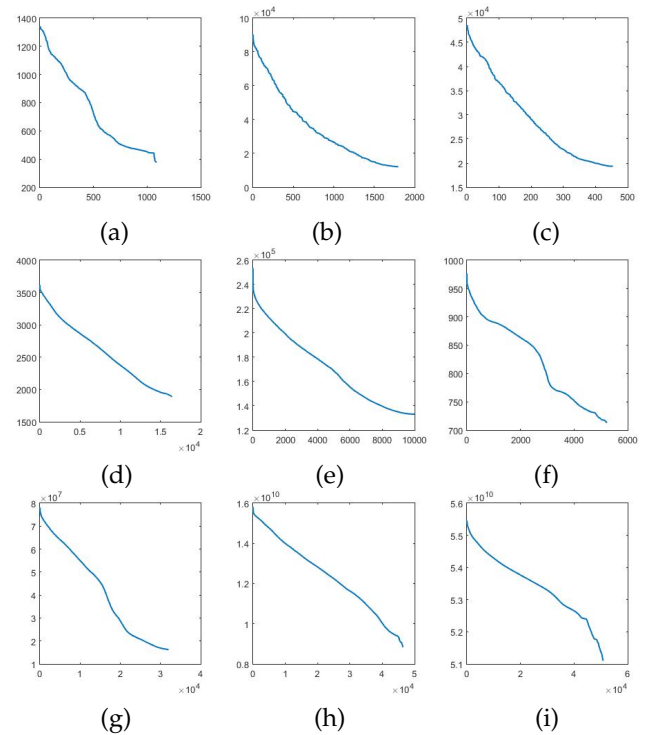


Fig. 5. Descent stability of MSAGP on 9 UCI datasets. (a) Glass. (b) Dermatology. (c) Breast-cancer. (d) Natural. (e) Waveform. (f) Yeast. (g) Satellite. (h) Yale-faces. (i) Epileptic.

4.4 Iteration Number of MSAGP and AGP

In this subsection, we compare iteration number for MSAGP and AGP ($t = 0.01$ and 0.1) to converge on 8 UCI datasets, including Segmentation, Parkinson, Dermatology, Breast-cancer, Seeds, Ionosphere, Glass and Iris. The results are illustrated in Figs. 6-7 and reported in Table 5, where we have the following observations.

TABLE 4
External Evaluation of PKM, KM++ and FCM ($m = 1.3$).

Datasets	NMI			ARI			VM		
	PKM	KM++	FCM	PKM	KM++	FCM	PKM	KM++	FCM
Yale-faces-B	0.7959	0.7952	0.7722	0.6631	0.6123	0.6386	0.8264	0.1744	0.0059
Iris	0.7501	0.6733	0.6723	0.7233	0.5779	0.5763	0.7419	0.7149	0.7081
Seeds	0.7025	0.7025	0.6949	0.7135	0.7135	0.7166	0.7050	0.6999	0.6949
Breast-cancer	0.7546	0.7478	0.7478	0.8521	0.8464	0.8464	0.7545	0.7478	0.7478
Dermatology	0.1141	0.1032	0.1046	0.0391	0.0266	0.0261	0.1140	0.1056	0.1095
Ionosphere	0.1349	0.1349	0.1299	0.1777	0.1777	0.1727	0.1348	0.1348	0.1298
Parkinson	0.1124	0.1217	0.1217	0.1876	0.2046	0.2046	0.1153	0.0607	0.1262
Glass	0.3294	0.4178	0.3489	0.2201	0.2551	0.2126	0.3871	0.3857	0.3807
Natural	0.0523	0.0536	0.0521	0.0247	0.0261	0.0273	0.0518	0.0529	0.0495
Satellite	0.6117	0.6117	0.5471	0.5292	0.5293	0.4289	0.5790	0.5544	0.6128
Yeast	0.0050	0.0050	0.0043	0.0117	0.0117	0.0109	0.0048	0.0045	0.0045
Segmentation	0.5338	0.5132	0.4678	0.3823	0.3313	0.3172	0.4996	0.5252	0.5729
Waveform	0.3622	0.3622	0.3606	0.2536	0.2536	0.2529	0.3622	0.3622	0.3559
Epileptic	0.1228	0.1675	0.0033	0.0245	0.0263	0.0025	0.1226	0.1291	0.0058

TABLE 5
Iteration number for MSAGP and AGP to converge with objective function value on 8 UCI datasets.

	Iteration number			Objective function value		
	MSAGP	AGP ($t = 0.01$)	AGP ($t = 0.1$)	MSAGP	AGP ($t = 0.01$)	AGP ($t = 0.1$)
Segmentation	1290	1338	1291	986167.4343	986167.4343	986167.4343
Parkinson	195	196	196	1343350.02	1343350.02	1343350.02
Dermatology	1801	6329	2247	11715.1043	11715.1041	11715.1043
Breast-cancer	452	577	462	19323.2	19323.2	19323.2
Seeds	421	634	534	587.32	587.32	587.32
Glass	1079	190683	115145	378.9	377.19	381.74
Ionosphere	368	2070	524	2419.3	2419.3	2419.3
Iris	308	53022	5573	78.95	78.95	78.95

1) MSAGP requires fewer iterations to converge than AGP on the eight datasets, especially much fewer on Dermatology (Fig. 6c), Ionosphere (Fig. 6f), Glass (Figs. 7a-c) and Iris (Figs. 7d-f).

2) When converging, MSAGP and AGP have the same objective function value on Parkinson, Breast-cancer, Seeds, Ionosphere and Iris. However, MSAGP has an objective function value slightly greater than AGP ($t = 0.01$) on Segmentation, Dermatology and Glass, while slightly smaller than AGP ($t = 0.1$) on Glass.

Overall, MSAGP can reach a competitive convergence with AGP in fewer iterations.

4.5 Convergence Speed of FMSAGP and MSAGP

In this subsection, we compare convergence speed of FMSAGP and MSAGP in running time on 9 UCI datasets: Parkinson, Iris, Seeds, Glass, Segmentation, Breast-cancer, Dermatology, Yeast and Waveform. The results are reported in Table 6, where we have the following observations.

1) FMSAGP runs faster than MSAGP on all the nine datasets.

2) The larger the dataset, the lower the speed-up (η) of FMSAGP to MSAGP. For example, the speed-up is 47.3% on Iris (150 samples), 22.3% on Glass (214 samples), 9.7% on Yeast (2426 samples) and 1.5% on Waveform (5000 samples).

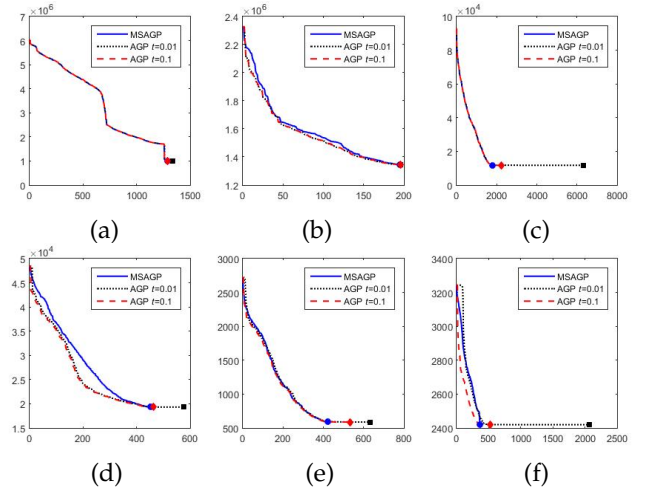


Fig. 6. Iteration number (in x-axis) for MSAGP and AGP ($t = 0.01$ and 0.1) to converge on 6 UCI datasets: Segmentation (a), Parkinson (b), Dermatology (c), Breast-cancer (d), Seeds (e) and Ionosphere (f). Y-axis means objective function value of PKM.

5 CONCLUSION

In this paper, the most important contribution is our solution to the clustering problem of FCM at $m = 1$ by a

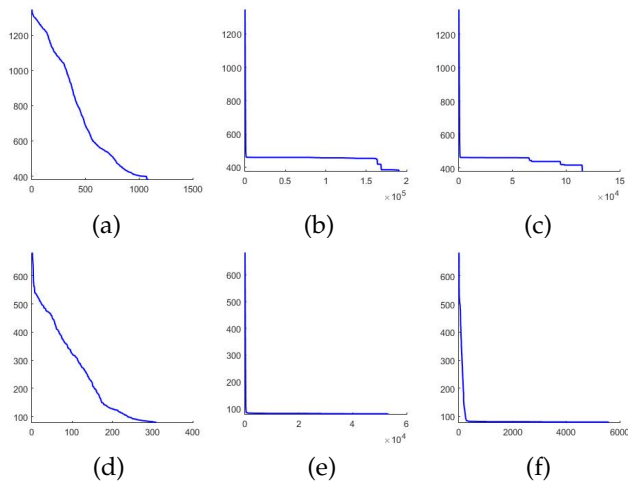


Fig. 7. Iteration number (in x-axis) for MSAGP (a) and AGP ($t = 0.01$) (b) AGP ($t = 0.1$) (c) to converge on Glass, and for MSAGP (d) and AGP ($t = 0.01$) (e) AGP ($t = 0.1$) (f) on Iris. Y-axis means objective function value of PKM.

TABLE 6
Running Time (s) of FMSAGP and MSAGP with speed-up on 9 UCI datasets.

	FMSAGP	MSAGP	η
Parkinson	0.1395	0.2895	48.2%
Iris	0.2691	0.5692	47.3%
Seeds	0.4868	1.3117	37.1%
Glass	2.4432	10.9369	22.3%
Segmentation	2.7152	14.6201	18.6%
Breast-cancer	0.8911	5.4898	16.2%
Dermatology	6.1486	40.7612	15.1%
Yeast	137.98	1418.47	9.7%
Waveform	173.49	11957.21	1.5%

new model, i.e. PKM. Moreover, we have addressed the PKM model by three methods: AGP, MSAGP and FMSAGP. Additionally, we have conducted a large number of experiments to evaluate how well these methods work in initialization robustness, clustering performance, descent stability, iteration number, and convergence speed. As future work, we will further improve our solution to PKM, and apply the basic idea to other relevant problems, like L_p -norm K-means, kernel PKM, and even possibilistic c-means. Particularly, we will combine deep neural networks [55], [56] with PKM to build deep PKM models, and to develop more nonlinear programming models for machine learning.

ACKNOWLEDGMENTS

This work was supported by the National Natural Science Foundation of China under grant numbers: 61876010 and 61806013.

REFERENCES

- Purkait P, Chin T J, Sadri A, et al. Clustering with Hypergraphs: The Case for Large Hyperedges[J]. IEEE Transactions on Pattern Analysis and Machine Intelligence, 2017, 39(9): 1697-1711.
- Otto C, Wang D, Jain A. Clustering Millions of Faces by Identity[J]. IEEE Transactions on Pattern Analysis and Machine Intelligence, 2018, 40(2):289-303.
- Kim S, Yoo C D, Nowozin S, et al. Image Segmentation Using Higher-Order Correlation Clustering[J]. IEEE Transactions on Pattern Analysis and Machine Intelligence, 2014, 36(9):1761-1774.
- Marin D, Tang M, Ayed I B, et al. Kernel Clustering: Density Biases and Solutions[J]. IEEE Transactions on Pattern Analysis and Machine Intelligence, 2019, 41(1):136-147.
- Heymann J, Drude L, Haeb-Umbach R. A Generic Neural Acoustic Beamforming Architecture for Robust Multi-Channel Speech Processing[J]. Computer Speech and Language, 2017, 46: 374-385.
- Ronan T, Qi Z, Naegle K M. Avoiding Common Pitfalls When Clustering Biological Data[J]. Science Signaling, 2016, 9(432):re6.
- Taylor M J, Husain K, Gartner Z J, et al. A DNA-Based T Cell Receptor Reveals a Role for Receptor Clustering in Ligand Discrimination[J]. Cell, 2017, 169(1):108-119.
- Liu A A, Su Y T, Nie W Z, et al. Hierarchical Clustering Multi-Task Learning for Joint Human Action Grouping and Recognition[J]. IEEE Transactions on Pattern Analysis and Machine Intelligence, 2016, 39(1):102-114.
- LI Y J. A Clustering Algorithm Based on Maximal θ -Distant Subtrees. Pattern Recognition. 2007, 40(5):1425-1431.
- Frey B J, Dueck D. Clustering by Passing Messages Between Data Points [J]. Science, 2007, 315(5814):972-976.
- Macqueen J. Some Methods for Classification and Analysis of Multivariate Observations[C]. Proc. of 5th Berkeley Symposium on Mathematical Statistics and Probability, 1967:281-297.
- Kaufmann L, Rousseeuw P J. Clustering by Means of Medoids[C]. Statistical Data Analysis Based on the L1-norm and Related Methods. North-Holland, 1987:405-416.
- Bezdek J C. Pattern Recognition with Fuzzy Objective Function Algorithms[M]. Plenum Press, 1981.
- Guha S, Rastogi R, Shim K, et al. CURE: An Efficient Clustering Algorithm for Large Databases[J]. Information Systems, 1998, 26(1):35-58.
- Madan S, Dana K J. Modified Balanced Iterative Reducing and Clustering Using Hierarchies (m-BIRCH) for Visual Clustering[J]. Pattern Analysis and Applications, 2016, 19(4):1023-1040.
- Johnson T, Singh S K. Divisive Hierarchical Bisecting MinCMax Clustering Algorithm[M]. Proceedings of the International Conference on Data Engineering and Communication Technology. 2017.
- Ester M, Kriegel H P, Xu X. A Density-Based Algorithm for Discovering Clusters in Large Spatial Databases with Noise[C]. International Conference on Knowledge Discovery and Data Mining, 1996:226-231.
- Rodriguez A, Laio A. Clustering by Fast Search and Find of Density Peaks[J]. Science, 2014, 344(6191):1492-1496.
- Szlam A, Bresson X. Total Variation and Cheeger Cuts[C]. International Conference on Machine Learning. 2010: 1039-1046.
- Elankavi R, Kalaiarasath R, Udayakumar R. A Fast Clustering Algorithm for High-Dimensional Data[J]. International Journal of Civil Engineering and Technology, 2017, 8(5):1220-1227.
- Luxburg U V. A Tutorial on Spectral Clustering[J]. Statistics and Computing, 2007, 17(4):395-416.
- Wu B, Wilamowski B M. A Fast Density and Grid Based Clustering Method for Data with Arbitrary Shapes and Noise[J]. IEEE Transactions on Industrial Informatics, 2016, 13(4):1620-1628.
- Sheikholeslami G, Chatterjee S, Zhang A. WaveCluster: A Wavelet-Based Clustering Approach for Spatial Data in Very Large Databases[J]. Vldb Journal, 2000, 8(3-4):289-304.
- Schikuta E. Grid-Clustering: An Efficient Hierarchical Clustering Method for Very Large Data Sets[C]. IEEE International Conference on Pattern Recognition, 1996, 2:101-105.
- Lin X, Soergel D, Marchionini G. A Self-Organizing Semantic Map for Information Retrieval[C]. ACM SIGIR conference on Research and development in information retrieval, 1991: 262-269.
- Rao S R, Yang A Y, Sastry S S, et al. Robust Algebraic Segmentation of Mixed Rigid-Body and Planar Motions from Two Views[J]. International Journal of Computer Vision, 2010, 88(3):425-446.
- Kadir S N, Goodman D F, Harris K D. High-Dimensional Cluster Analysis with The Masked Em Algorithm[J]. Neural Computation, 2014, 26(11):2379-2394.
- Elhamifar E, Vidal R. Sparse Subspace Clustering[C]. IEEE Conference on Computer Vision and Pattern Recognition, 2009:2790-2797.

- [29] Lu C, Feng J, Lin Z, et al. Subspace Clustering by Block Diagonal Representation[J]. IEEE Transactions on Pattern Analysis and Machine Intelligence, 2018, 41(2):487-501.
- [30] Chen J, Li Z, Huang B. Linear Spectral Clustering Superpixel[J]. IEEE Transactions on Image Processing, 2017, 26(7):3317-3330.
- [31] Nie F, Wang X, Huang H. Clustering and Projected Clustering with Adaptive Neighbors[C]. ACM International Conference on Knowledge Discovery and Data Mining, 2014:977-986.
- [32] Kearns M, Mansour Y, Ng A. An Information-Theoretic Analysis of Hard and Soft Assignment Methods for Clustering[C]. Uncertainty in Artificial Intelligence, 1997.
- [33] Lloyd S. Least Squares Quantization In PCM[J]. IEEE transactions on information theory, 1982, 28(2):129-137.
- [34] Hartigan J A, Wong M A. Algorithm AS 136: A K-Means Clustering Algorithm[J]. Journal of the Royal Statistical Society, 1979, 28(1):100-108.
- [35] Laszlo M, Mukherjee S. A Genetic Algorithm Using Hyper-Quadrees for Low-Dimensional K-Means Clustering[J]. IEEE Transactions on Pattern Analysis and Machine Intelligence, 2006, 28(4):533-543.
- [36] Arthur D, Vassilvitskii S. K-means++: The Advantages of Careful Seeding[C]. Society for Industrial and Applied Mathematics, 2007, 11(6):1027-1035.
- [37] Selim S and Ismail M. K-Means-Type Algorithms: A Generalized Convergence Theorem and Characterization of Local Optimality[J]. IEEE Transactions on Pattern Analysis and Machine Intelligence, 1984, 6(1):81-87.
- [38] Su M C, Chou C H. A Modified Version of the K-Means Algorithm with a Distance Based on Cluster Symmetry[J]. IEEE Transactions on Pattern Analysis and Machine Intelligence, 2001, 23(6):674-680.
- [39] Yu S, Tranchevent L C, Liu X, et al. Optimized Data Fusion for Kernel K-Means Clustering[J]. IEEE Transactions on Pattern Analysis and Machine Intelligence, 2012, 34(5):1031-1039.
- [40] Huang X and Ye Y and Zhang H. Extensions of Kmeans-Type Algorithms: A New Clustering Framework by Integrating Intracluster Compactness and Intercluster Separation[J]. IEEE Transactions on Neural Networks and Learning Systems. 2014, 25(8):1433-1446.
- [41] Pal N R, Bezdek J C. On Cluster Validity for The Fuzzy C-Means Model[J]. IEEE Transactions on Fuzzy Systems, 1995, 3(3):370-379.
- [42] Krishnapuram R, Keller J M. The Possibilistic C-Means Algorithm: Insights and Recommendations[J]. IEEE Transactions on Fuzzy Systems, 1996, 4(3):385-393.
- [43] Koutroumbas K D, Xenaki S D, Rontogiannis A A. On the Convergence of the Sparse Possibilistic C-Means Algorithm[J]. IEEE Transactions on Fuzzy Systems, 2018, 26(1):324-337.
- [44] Lin P L, Huang P W, Kuo C H, et al. A Size-Insensitive Integrity-Based Fuzzy C-Means Method for Data Clustering[J]. Pattern Recognition, 2014, 47(5):2042-2056.
- [45] Nocedal J, Wright S. Numerical Optimization[M]. Springer Science and Business Media, 2006.
- [46] Rosen J B. The Gradient Projection Method for Nonlinear Programming. Part I. Linear Constraints[J]. Journal of the Society for Industrial and Applied Mathematics, 1961, 9(4):514-532.
- [47] Goldfarb D, Lapidus L. Conjugate Gradient Method for Nonlinear Programming Problems with Linear Constraints[J]. Industrial and Engineering Chemistry Fundamentals, 1968, 7(1):142-151.
- [48] Duda R O, Hart P E, Stork D G. Pattern Classification: 2nd Edition[M]. Wiley and Sons, 2001.
- [49] Zhang X D. Matrix Analysis and Applications[M]. Tsinghua University Press, 2004:681-682.
- [50] Honig M, Madhow U, Verdu S. Blind Adaptive Multiuser Detection[J]. IEEE Transactions on Information Theory, 1995, 41(4):944-960.
- [51] Shores T S. Applied Linear Algebra and Matrix Analysis: 2nd ed[M]. Undergraduate Texts in Mathematics, 2007.
- [52] Davies D L, Bouldin D W. A Cluster Separation Measure[J]. IEEE Transactions on Pattern Analysis and Machine Intelligence, 1979, 1(2):224-227.
- [53] Vinh N X, Epps J, Bailey J. Information Theoretic Measures for Clusterings Comparison: Variants, Properties, Normalization and Correction for Chance[J]. Journal of Machine Learning Research, 2010, 11(1):2837-2854.
- [54] Rosenberg A, Hirschberg J. V-measure: A Conditional Entropy-Based External Cluster Evaluation Measure[C]. Empirical Methods in Natural Language Processing and Computational Natural Language Learning, 2007, 410-420.
- [55] Lecun Y, Bengio Y, Hinton G. Deep learning[J]. Nature, 2015, 521(7553):436.
- [56] Li Y, Zhang T. Deep neural mapping support vector machines[J]. Neural Networks, 2017, 93:185-194.



Yujian Li has been with College of Computer Science, Beijing University of Technology since 2001, and with School of Artificial Intelligence, Guilin University of Electronic Technology since 2019. He received the BS degree from Department of Applied Mathematics, Huazhong University of Science and Technology in 1990, and the MS degree from Institute of Mathematics, Chinese Academy of Sciences in 1993, and the PhD degree from Institute of Semiconductors, Chinese Academy of Sciences in 1999. From 1993 to 1996, he was with Institute of Biophysics, Chinese Academy of Sciences. From 1999 to 2001, he was a post-doctoral fellow in the Beijing University of Posts and Telecommunications. His current research interests include deep learning, pattern analysis, machine intelligence, and image processing.



Bowen Liu is a doctoral candidate in the Faculty of Information Technology, Beijing University of Technology (BJUT). His research interests include clustering and machine learning.



Zhaoying Liu born in 1986. PhD, lecturer, master supervisor. Member of China Computer Federation (CCF) and Chinese Association for Artificial Intelligence (CAAI), currently works in the Faculty of Information Technology, Beijing University of Technology (BJUT). She received her Ph. D from Beihang University in 2015. Her main research interests include image processing, pattern recognition, and deep learning.



Ting Zhang received her PhD degree from the College of Computer Science of Beijing University of Technology in 2018. She is currently a Post-doctor in the Faculty of Information Technology of Beijing University of Technology. Member of China Computer Federation (CCF). Her current research interests include pattern recognition, deep learning, and machine learning.